

## **Supporting Information**

# **Robust InNCo<sub>3-x</sub>Mn<sub>x</sub> Nitride Supported Pt Nanoparticles as High Performance Bifunctional Electrocatalysts for Zn-Air Batteries**

Li Du,<sup>†a</sup> Mengyuan Lv,<sup>†a</sup> Jiaxi Zhang,<sup>a</sup> Huiyu Song,<sup>a</sup> Dai Dang,<sup>b</sup> Quanbing Liu,<sup>b,\*</sup>

Zhiming Cui<sup>a,\*</sup> and Shijun Liao<sup>a</sup>

- a. The Key Laboratory of Fuel Cell Technology of Guangdong Province, School of Chemistry and Chemical Engineering, South China University of Technology, Guangzhou 510641, China.
- b. School of Chemical Engineering and Light Industry, Guangdong University of Technology, Guangzhou 510006, China

† Both authors contributed equally to this work.

Corresponding Author:

E-mail address: a\*.zmcui@scut.edu.cn; b\*.liuqb@gdut.edu.cn

## **Table of contents**

**S1. X-Ray Powder Diffraction**

**S2. OER polarization curves for InNCo<sub>3</sub> and Mn-doped samples**

**Table S1. OER activity comparison**

**S3. Tafel slope**

**S4. Electrochemical impedance spectroscopy (EIS)**

**S5. ECSA normalized polarization curves**

**References**

## S1. X-Ray Powder Diffraction

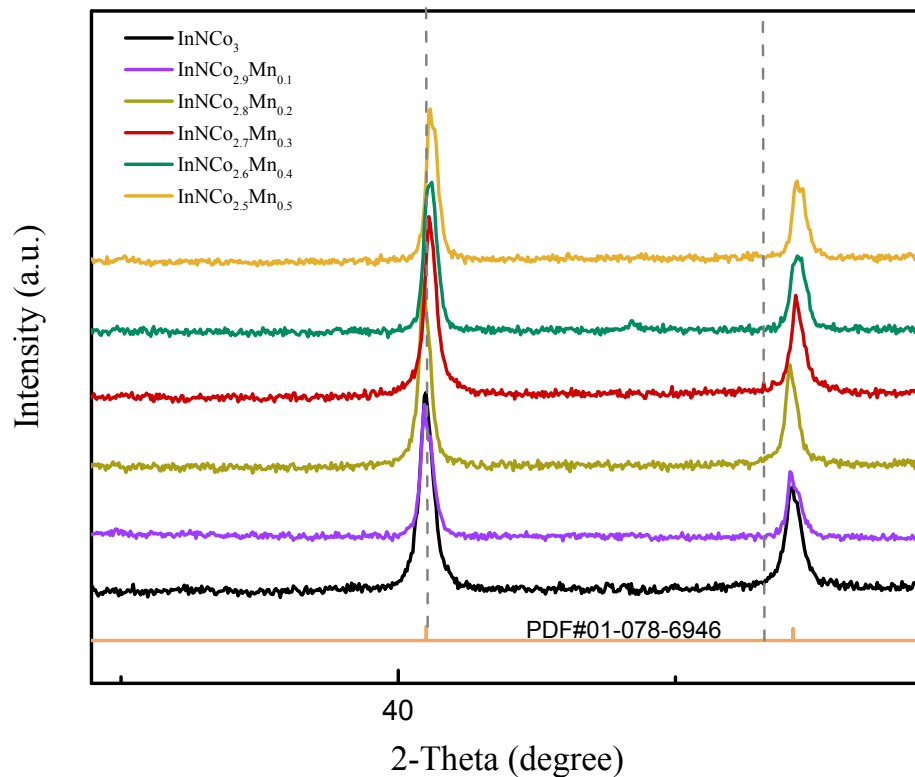


**Figure. S1.** The doping of Mn atoms results in XRD peaks shift towards higher angles, suggesting the partial substitution of Co by the smaller atom Mn. In addition, the  $2\theta$  values have more positive shift with further increasing the amount of Mn.

## S2. OER polarization curves for $\text{InNC}\text{o}_3$ and Mn-doped samples

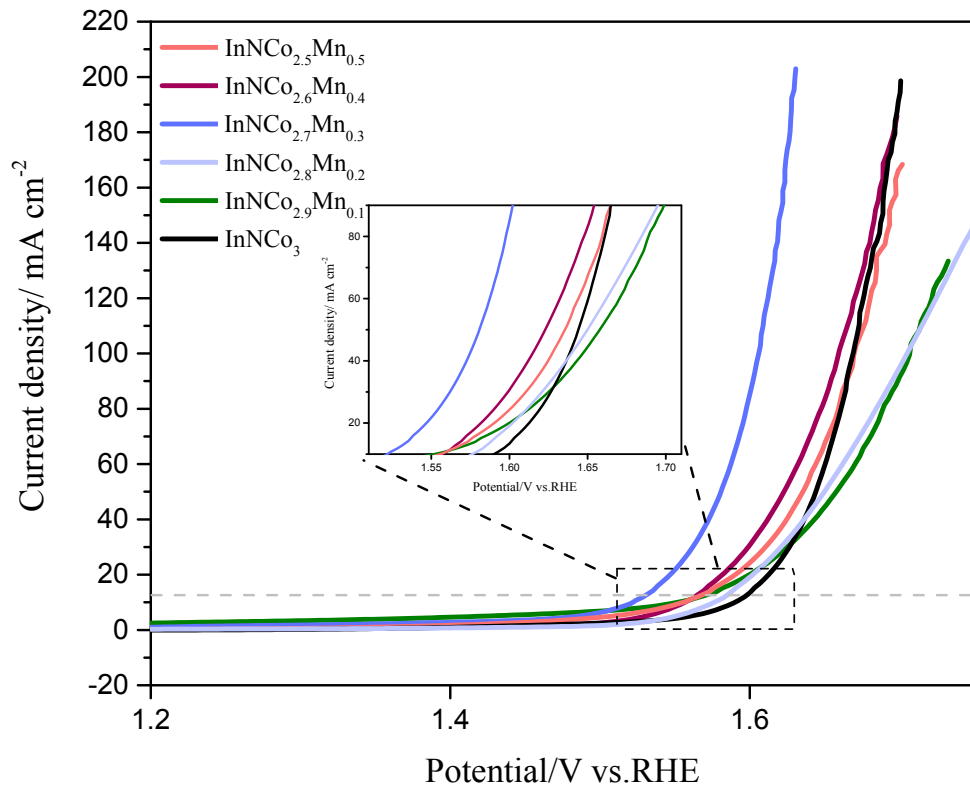


**Figure. S2.** OER polarization curves for  $\text{InNC}\text{o}_3$  and all the Mn-doped samples tests in 1M KOH solution. The OER plots have been zoomed to compare the overpotentials at 10  $\text{mA cm}^{-2}$ . The linear-sweep voltammograms (LSV) were after IR correction. It shows that doping Mn can greatly enhance the OER activity, which  $\text{InNC}\text{o}_{2.7}\text{Mn}_{0.3}$  demonstrated the lowest overpotential of 300 mV to reach the current density at 10  $\text{mA cm}^{-2}$ , followed by  $\text{InNC}\text{o}_{2.6}\text{Mn}_{0.4}$  (323 mV),  $\text{InNC}\text{o}_{2.5}\text{Mn}_{0.5}$  (327 mV),  $\text{InNC}\text{o}_{2.9}\text{Mn}_{0.1}$  (322 mV),  $\text{InNC}\text{o}_{2.8}\text{Mn}_{0.2}$  (344 mV) and  $\text{InNC}\text{o}_3$  (360 mV).

**Table S1. OER activity comparison**

**Table S1.** (OER activity comparison of as-prepared anti-perovskite InNCo<sub>3</sub> and Mn-doped samples with other superior non-noble OER catalysts previously reported.

Catalyst	Overpotentials (mV)	Tafel slop (mV dec <sup>-1</sup> )	Electrolyte concentration	Reference
<b>InNCo<sub>3</sub></b>	<b>360</b>	<b>85</b>	1M KOH	<b>this work</b>
<b>InNCo<sub>2.5</sub>Mn<sub>0.5</sub></b>	<b>327</b>	<b>115</b>	1M KOH	<b>this work</b>
<b>InNCo<sub>2.6</sub>Mn<sub>0.4</sub></b>	<b>323</b>	<b>87</b>	1M KOH	<b>this work</b>
<b>InNCo<sub>2.7</sub>Mn<sub>0.3</sub></b>	<b>300</b>	<b>84</b>	1M KOH	<b>this work</b>
<b>InNCo<sub>2.8</sub>Mn<sub>0.2</sub></b>	<b>344</b>	<b>91</b>	1M KOH	<b>this work</b>
<b>InNCo<sub>2.9</sub>Mn<sub>0.1</sub></b>	<b>322</b>	<b>148</b>	1M KOH	<b>this work</b>
CoN	290	70	1M KOH	1
Co <sub>4</sub> N/CNW/CC	310	81	1M KOH	2
CoP/CN	300	68	1M KOH	3
CoSn <sub>2</sub> /FTO	299	89	1M KOH	4
Ni <sub>3</sub> Ge <sub>2</sub> O <sub>5</sub> (OH) <sub>4</sub>	320	67.5	1M KOH	5
MnO <sub>2</sub> -0.5IL	394	49	1M KOH	6
P-Co-NC-4	315	75.7	1M KOH	7
Ni-MnO/rGO	370	67	0.1M KOH	8
BCFSn-721	300	69	0.1M KOH	9

NiCo-LDH-G	337	52	0.1M KOH	10
Co-N, B-CSs	430	-	0.1M KOH	11
LCF-700	293	67	0.1M KOH	12

### S3. Tafel slope

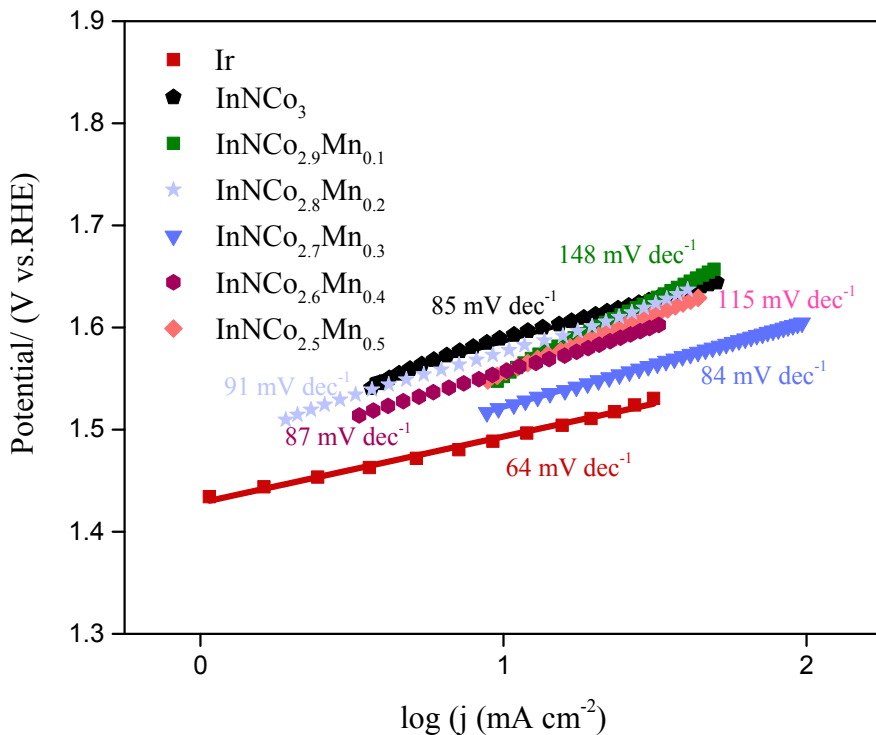


**Figure. S3.** Tafel slopes of as-prepared anti-perovskite nitride samples and commercial Ir/C. This comparison clearly showed that doping Mn can significantly improve the OER performance and electronic conductivity as well, thus leading to a faster reaction. InNCo<sub>3</sub> yields a competitively high Tafel slop of 85 mV dec<sup>-1</sup> while InNCo<sub>2.7</sub>Mn<sub>0.3</sub> shows a similarly Tafel slop of 84 mV dec<sup>-1</sup>. The Tafel slop of InNCo<sub>2.6</sub>Mn<sub>0.4</sub>, InNCo<sub>2.8</sub>Mn<sub>0.2</sub> InNCo<sub>2.5</sub>Mn<sub>0.5</sub> and InNCo<sub>2.9</sub>Mn<sub>0.1</sub> are 87 mV dec<sup>-1</sup>, 91 mV dec<sup>-1</sup>, 115 mV dec<sup>-1</sup> and 148 mV dec<sup>-1</sup>, respectively.

## S4. Electrochemical impedance spectroscopy (EIS)

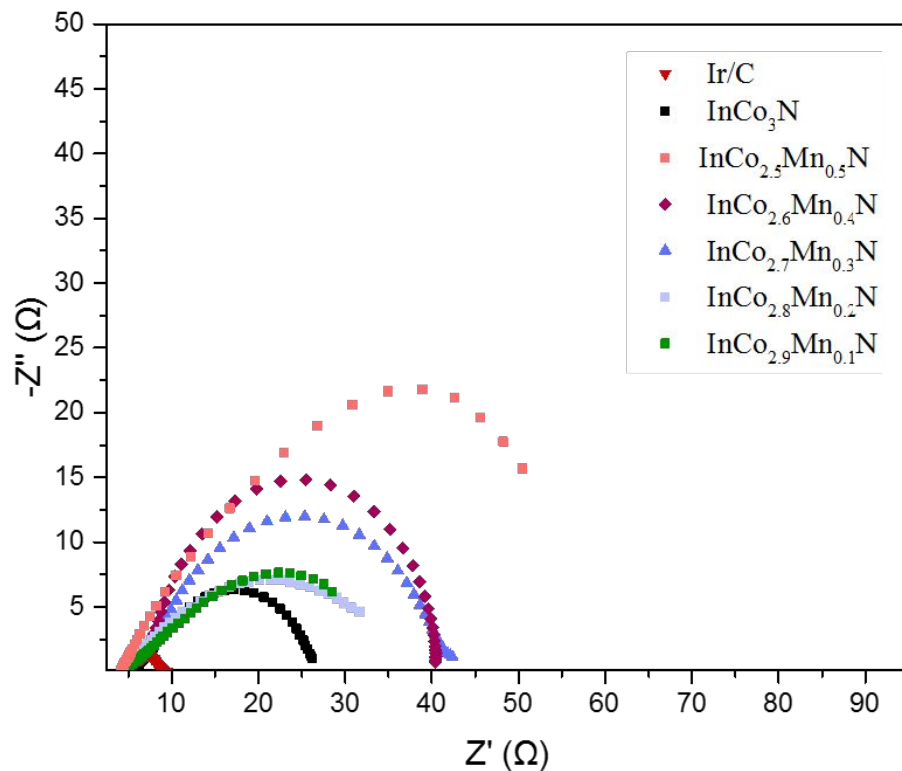


**Figure. S4.** The Nyquist plots of as-prepared anti-perovskite nitride samples and commercial Ir/C. The resistance of the solution was around 5.36, which can be observed from the X intercept. The radius of the semicircles represented the charge-transfer resistance  $R_{ct}$ . The  $R_{ct}$  of InNCo<sub>3</sub> was 10.33, much smaller than InNCo<sub>2.7</sub>Mn<sub>0.3</sub> (18.5), InNCo<sub>2.95</sub>Mn<sub>0.05</sub> (18.7) and InNCo<sub>2.9</sub>Mn<sub>0.1</sub> (37.5), indicating a lower resistance.

## S5. ECSA normalized polarization curves

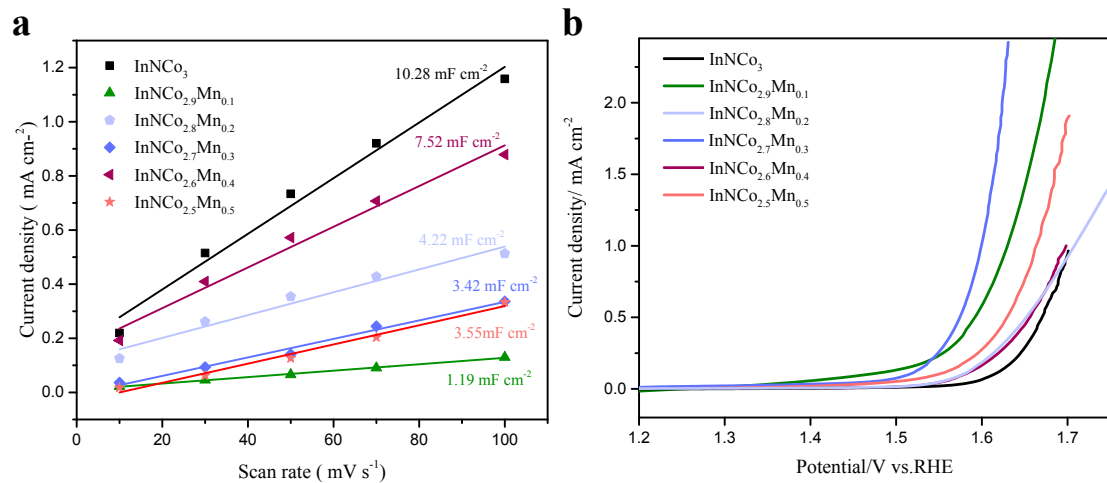


**Figure. S5.** (a) The  $C_{dl}$  values of InNCo<sub>3-x</sub>Mn<sub>x</sub> measured by the CV scan between 1.3 V and 1.4 V (vs. RHE) under different scan rate of 10 mV s<sup>-1</sup>, 30 mV s<sup>-1</sup>, 50 mV s<sup>-1</sup>, 70 mV s<sup>-1</sup> and 100 mV s<sup>-1</sup>. (b) ECSA normalized polarization curves for the as-prepared anti-perovskite nitrides samples.

## References

1. Zhang, Y. Q.; Ouyang, B.; Xu, J.; Jia, G. C.; Chen, S.; Rawat, R. S.; Fan, H. J., Rapid Synthesis of Cobalt Nitride Nanowires: Highly Efficient and Low-Cost Catalysts for Oxygen Evolution. *Angew. Chem., Int. Edit.* **2016**, *55*, 8670-8674.
2. Meng, F. L.; Zhong, H. X.; Bao, D.; Yan, J. M.; Zhang, X. B., In Situ Coupling of Strung Co<sub>4</sub>N and Intertwined N-C Fibers toward Free-Standing Bifunctional Cathode for Robust, Efficient, and Flexible Zn Air-Batteries. *J. Am. Chem. Soc.* **2016**, *138*, 10226-10231.
3. Weng, B. C.; Wei, W.; Yiliguma; Wu, H.; Alenizi, A. M.; Zheng, G. F., Bifunctional CoP and CoN porous nanocatalysts derived from ZIF-67 in situ grown on nanowire photoelectrodes for efficient photoelectrochemical water splitting and CO<sub>2</sub> reduction. *J. Mater. Chem. A* **2016**, *4*, 15353-15360.
4. Menezes, P. W.; Panda, C.; Garai, S.; Walter, C.; Guiet, A.; Driess, M., Structurally Ordered Intermetallic Cobalt Stannide Nanocrystals for High-Performance Electrocatalytic Overall Water-Splitting. *Angew. Chem., Int. Edit.* **2018**, *57*, 15237-15242.
5. Zhang, N.; Yang, B. P.; He, Y. Q.; He, Y. L.; Liu, X. H.; Liu, M.; Song, G. Y.; Chen, G.; Pan, A. Q.; Liang, S. Q.; Ma, R. Z.; Venkatesh, S.; Roy, V. A. L., Serpentine Ni<sub>3</sub>Ge<sub>2</sub>O<sub>5</sub>(OH)<sub>4</sub> Nanosheets with Tailored Layers and Size for Efficient Oxygen Evolution Reactions. *Small* **2018**, *14*, 8.
6. Yan, G. B.; Lian, Y. B.; Gu, Y. D.; Yang, C.; Sun, H.; Mu, Q. Q.; Li, Q.; Zhu, W.; Zheng, X. S.; Chen, M. Z.; Zhu, J. F.; Deng, Z.; Peng, Y., Phase and Morphology

Transformation of MnO<sub>2</sub> Induced by Ionic Liquids toward Efficient Water Oxidation.

*ACS Catal.* **2018**, *8*, 10137-10147.

7. Liang, Z. Z.; Zhang, C. C.; Yuan, H. T.; Zhang, W.; Zheng, H. Q.; Cao, R., PVP-assisted transformation of a metal-organic framework into Co-embedded N-enriched meso/microporous carbon materials as bifunctional electrocatalysts. *Chem. Commun.* **2018**, *54*, 7519-7522.
8. Fu, G. T.; Yan, X. X.; Chen, Y. F.; Xu, L.; Sun, D. M.; Lee, J. M.; Tang, Y. W., Boosting Bifunctional Oxygen Electrocatalysis with 3D Graphene Aerogel-Supported Ni/MnO Particles. *Adv. Mater.* **2018**, *30*, 1704609.
9. Xu, X. M.; Su, C.; Zhou, W.; Zhu, Y. L.; Chen, Y. B.; Shao, Z. P., Co-doping Strategy for Developing Perovskite Oxides as Highly Efficient Electrocatalysts for Oxygen Evolution Reaction. *Adv. Sci.* **2016**, *3* (2), 1500187.
10. Yang, J.; Yu, C.; Hu, C.; Wang, M.; Li, S. F.; Huang, H. W.; Bustillo, K.; Han, X. T.; Zhao, C. T.; Guo, W.; Zeng, Z. Y.; Zheng, H. M.; Qiu, J. S., Surface-Confined Fabrication of Ultrathin Nickel Cobalt-Layered Double Hydroxide Nanosheets for High-Performance Supercapacitors. *Adv. Funct. Mater.* **2018**, *28* (44), 1803272.
11. Guo, Y. Y.; Yuan, P. F.; Zhang, J. N.; Hu, Y. F.; Amiinu, I. S.; Wang, X.; Zhou, J. G.; Xia, H. C.; Song, Z. B.; Xu, Q.; Mu, S. C., Carbon Nanosheets Containing Discrete Co-N-x-B-y-C Active Sites for Efficient Oxygen Electrocatalysis and Rechargeable Zn-Air Batteries. *Acs Nano* **2018**, *12*, 1894-1901.
12. Song, S. Z.; Zhou, J.; Su, X. Z.; Wang, Y.; Li, J.; Zhang, L. J.; Xiao, G. P.; Guan, C. Z.; Liu, R. D.; Chen, S. G.; Lin, H. J.; Zhang, S.; Wang, J. Q., Operando X-ray

spectroscopic tracking of self-reconstruction for anchored nanoparticles as high-performance electrocatalysts towards oxygen evolution. *Energy Environ. Sci.* **2018**, *11*, 2945-2953.